The Journal of Engineering

WILEY

The Institution of Engineering and Technology

LETTER OPEN ACCESS

A Wideband Circularly Polarised Magneto-Electric Dipole Antenna Array With a Series Sequential Phase Feed Network

Elmien Coetzer | Johan Joubert | Johann Wilhelm Odendaal

Department of Electrical, Electronic and Computer Engineering, University of Pretoria, Pretoria, South Africa

Correspondence: Johan Joubert (jjoubert@up.ac.za)

Received: 29 April 2025 | **Revised:** 8 September 2025 | **Accepted:** 23 September 2025

Funding: The work was performed with internal university funding.

ABSTRACT

A printed circularly polarised antenna array is presented that utilizes the inherent good bandwidth and stable gain of magneto-electric dipoles in combination with the wideband benefits of a sequential rotation feed technique. The proposed antenna has a simple geometry using two substrates and does not require any additional cavity or parasitic elements. The designed and simulated antenna has an impedance bandwidth of more than 75%, a 3 dB axial ratio bandwidth of 67% and a peak gain of 12.4 dBic, with less than 3 dB gain variation across the entire axial ratio bandwidth. The antenna provides a good combination of simple and compact geometry, wide bandwidth, good gain and stable radiation patterns when compared to previously published research. Simulated as well as measured results are presented for a protype antenna array.

1 | Introduction

There is a growing need for antennas with wide bandwidth and stable high gain that can accommodate the demand for reliable communication systems that require large data rates and capacities, improved signal stability and low latency [1]. Circularly polarised (CP) antennas can improve polarisation mismatches and provide resistance towards multipath reflections and hence contribute to more stable and robust communication [1].

Many single-fed CP radiating elements have narrow axial ratio (AR) bandwidths. A sequential rotation (SR) technique [2] can be used to feed multiple geometrically rotated radiators with sequential phase (SP) to allow the design of small CP arrays (typically 2×2) with wider impedance bandwidth (IBW), AR bandwidth (ARBW) and gain bandwidth (GBW).

Several SR-fed CP antenna array designs using different types of radiating elements have been published. In [3] a low profile microstrip antenna is proposed that utilizes four linearly polarised (LP) patch radiators and achieved an IBW ($|s_{11}| \leq -10$ dB), ARBW (AR ≤ 3 dB) and maximum gain of 13.6%, 11.2% and 9.8 dBic. A similar feed network was used for four CP dielectric resonant antennas (DRA) in [4], and an IWB, ARBW and maximum gain of 53.7%, 51.1% and 12.6 dBic were achieved. The 3 dB GBW of this array was 45%, slightly less than the ARBW. In [5] a SR-fed 2×2 array of printed monopoles achieved an ARBW of 92.5%, a 3 dB GBW of 72.3% and a maximum gain of 12.6 dBic using an artificial magnetic conductor (AMC) consisting of a metal cone and an additional printed metasurface dielectric layer. The electric size of this antenna is $1.44\lambda_L \times 1.44\lambda_L \times 0.13\lambda_L$ (with λ_L the wavelength at the lowest frequency of the 3 dB GBW).

Crossed dipoles as radiating elements can also be used to realise low profile CP antennas with good bandwidth properties. A single substrate printed crossed dipole above a ground plane in [6] achieved a usable 3 dB GBW of 57.7% and a very stable average gain of 7.7 dBic, and another printed crossed dipole antenna

with an irregular ground plane and an additional dielectric layer above the ground plane [7] achieved a usable 3 dB GBW of 53.6% and a maximum gain of 11.3 dBic. In [8] and [9] more complex crossed dipole antenna structures are proposed (with square metal columns to generate an additional resonance, or a complex box-shaped cavity) to obtain very wide ARBWs of 94.4% and 121.2%, respectively. Because of the very compact size of the antenna presented in [8] (only $0.47\lambda_L \times 0.47\lambda_L \times 0.12\lambda_L$), the maximum gain achieved was only 7.9 dBic. The antenna presented in [9] exhibit very good ARBW but unstable radiation patterns from at least 5.3 GHz, with high sidelobes and cross-polarisation, and some squint. The effect of this can also be seen in the gain vs frequency response of the antenna. The antenna exhibits a dual 3 dB GBW behaviour, with the primary band (2.68–5.19 GHz, 63.7%) having a peak gain of 10.9 dBic, and reasonably stable radiation properties. There is then a secondary 3 dB GBW of 20.5% with a maximum gain of 12.6 dBic, but with compromised radiation patterns.

Magneto-electric (ME) dipole antennas have excellent characteristics including wide bandwidth, stable gain, low back-lobe radiation, low cross polarisation, and symmetrical radiation patterns over a wide bandwidth [10]. CP ME dipole antennas have been designed by modifying the shape or feed structure of the dipole elements. In [11] an antenna design is proposed that utilizes a single ME dipole with trapezoidal horizontal plates, a Γ-shaped feeding structure and a box shaped cavity to obtain an ARBW of 41%. In [1] two printed crossed ME dipoles is proposed, and achieved an IBW, ARBW and maximum gain of 70.2%, 51.5% and 9.9 dBic. This antenna also had stable gain over the entire ARBW, with a 51.5% usable 3 dB GBW.

A new printed CP ME dipole antenna with a simple geometry is presented in this paper, utilizing the benefits of the SR technique and the excellent characteristics of ME dipole antennas. A single printed proximity-coupled fed CP ME dipole was designed, and four of these dipoles where then combined using a series SP feed network. The new antenna has a good combination of simple and compact geometry, wide bandwidth, good gain and stable radiation patterns when compared to previously published research.

2 | Antenna Design

The two-layer substrate geometry of the new printed CP ME dipole array that was designed for a centre frequency $f_0 = 4$ GHz is shown in Figure 1a. The CP ME dipoles are printed on the bottom of the upper substrate, as shown in Figure 1b. Four semi-rigid coaxial feed lines with an outer radius of 1.1 mm were used to connect the output ports of the SP feed network (on the bottom substrate, see Figure 1d) to the printed proximity coupled T-shaped feeding strips of the four individual CP ME dipoles (on the top substrate, see Figure 1c). Four conducting DC shorting posts [10] with the same outer dimensions as the coaxial feed lines are also included and can also be seen in Figure 1a. A Rogers RO4003C substrate with ε_r= 3.38, tan δ = 0.0021 and T_1 = 1.524 mm was used as the upper substrate and another Rogers RO4003C substrate with ε_r= 3.38, tan δ = 0.0021 and T_2 = 0.813 mm was used as the lower substrate. The dimensions of the final design are presented in Table 1.

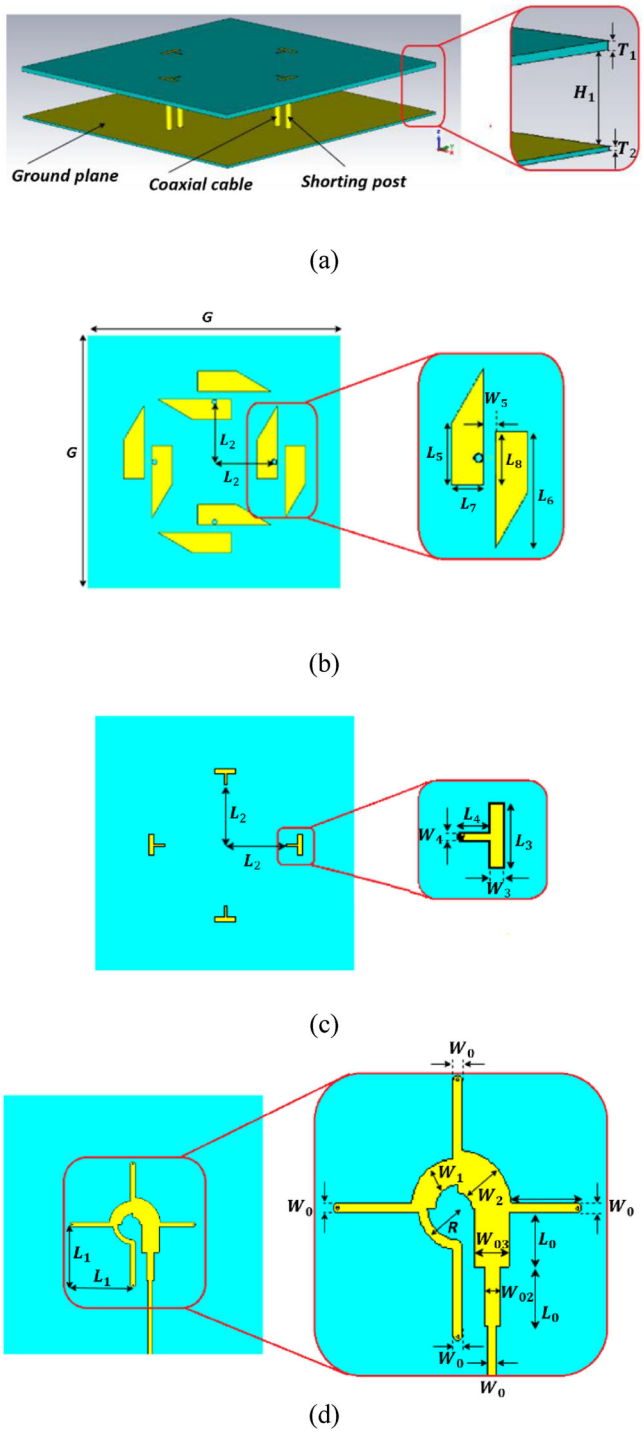

FIGURE 1 | Proposed array: (a) printed CP ME dipole array, (b) CP ME dipoles, (c) proximity coupled feeding strips, and (d) series SP feed network.

Previous designs of a printed LP ME dipole [10] and a modified CP ME dipole consisting of two pairs of vertical and trapezoidal copper plates and a metallic reflector with defected sidewalls [11] were used as basis to design a single printed CP ME dipole using CST Studio Suite as simulation tool. The new printed version of the CP ME dipole has two arms of which the ends have a trapezoidal shape, and a proximity coupled T-shaped feeding strip. The two halves of the electric dipole (trapezoidal shapes) of each single CP ME dipole are printed on the bottom

TABLE 1 | Dimensions of the proposed antenna.

Antenna dimensions (mm)					
G	100	L_3	8	W_{03}	6.8
T_1	1.524	L_4	4	W_1	4.8
T_2	0.813	L_5	15	W_2	7.8
H_1	16	L_6	28.5	W_3	2
R	6.7	L_7	8	W_4	1
L_0	10.7	L_8	13	W_5	3
L_1	16.5	W_0	1.81	ε_r	3.38
L_2	26	W_{02}	3		

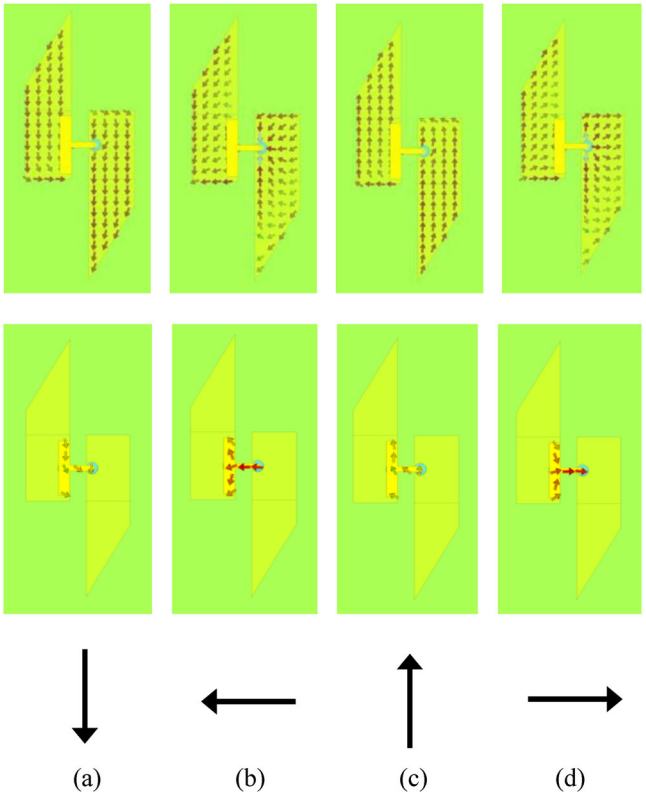

FIGURE 2 | Simulated electric current distributions at 4 GHz on the dipole arms and feeding strip of a single CP ME dipole, and the dominant polarization, at different time phases: (a) 0°, (b) 90°, (c) 180° and (d) 270°.

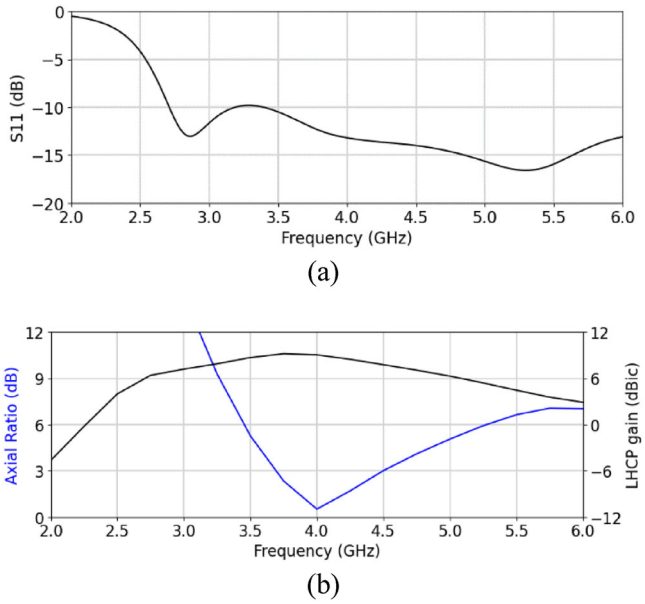

FIGURE 3 | Simulated results for the single CP ME dipole. (a) S_{11}; (b) gain and AR.

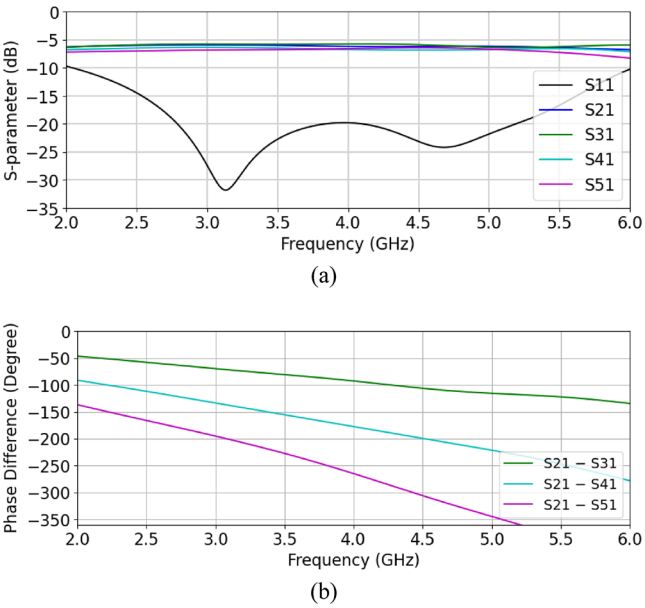

FIGURE 4 | Simulated S-parameters of the feed network: (a) magnitude and (b) phase difference.

side of the upper substrate (see Figure 1b) while the magnetic dipole is represented by the slot between the electric dipoles and a cavity between the printed dipoles and the reflector. CP is achieved because the directions of the electric field vectors of the electric and magnetic dipoles are oriented at a 90° angle and are effectively fed with a 90° phase difference. The proximity-coupled feeding strip, shown in Figure 1c, is printed on the top side of the upper substrate. As illustration of the orientation and phase of the electric currents, the simulated current distributions at different time phases on a single CP ME dipole are shown in Figure 2a–d. The dominant polarization of the radiator is also shown at each time interval. The horizontal electrical field component produced by the magnetic dipole (excited by the horizontal current on the feeding strip) lags the vertical electric field component (produced by the electric currents on the electric dipole), causing a circularly polarized radiated field.

The simulated reflection coefficient of a single printed CP ME dipole is shown in Figure 3a, and the simulated gain and AR are shown in Figure 3b. The antenna achieved an IBW >75%, an ARBW >19% and a maximum gain 9.1 dBic. This single CP ME dipole antenna also had stable gain over a wide bandwidth.

To improve the CP bandwidth and gain, a CP ME dipole array was formed by combining four geometrically rotated single, printed CP ME dipoles using a SP feed network. The series SP feed network based on [12] uses a stepped impedance transmission

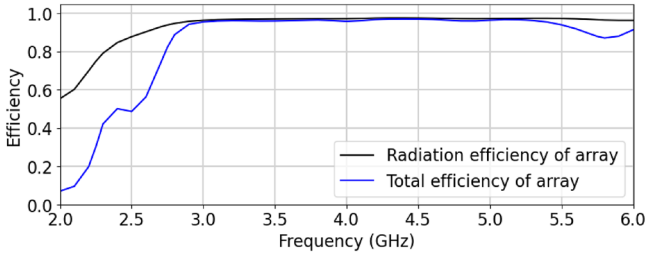

FIGURE 5 | Simulated efficiency of the CP ME dipole array.

line series power divider in an open ring configuration and a two-section quarter wave matching network to implement sequential-phase rotation and is printed on the bottom side of the lower substrate, as shown in Figure 1d. To improve the impedance matching bandwidth a two-section quarter wave matching network was implemented, with lengths L_0, and widths W_{02} and W_{03}. Final optimized dimensions are given in Table 1.

The simulated s-parameters (magnitude, and phase difference between the four output ports) of the final design are shown in Figures 4a and 4b. The feed network was implemented on a thin substrate with thickness $T_2 = 0.813$ mm to limit the microstrip line widths of the low impedance sections of the design. The simulated s-parameter balance for the feed network was better than 0.94 for the entire frequency range, which is an indication that the power losses due to radiation or dissipation in the substrate or conductors are relatively small. The reflection coefficient was <−15 dB and the magnitudes of the output port transmission coefficients were also well matched over the entire 2.5–5.5 GHz range. As expected, the phase differences between the output ports for such a series feed varied with frequency. The phase delay between successive ports was on the order of 90° ± 35° over the 2.5–5.5 GHz range and would certainly be a limiting factor for good AR performance at the outer edges of the frequency band.

The design of the single CP ME dipole element and the dipole array were performed thorough simulation and optimization of

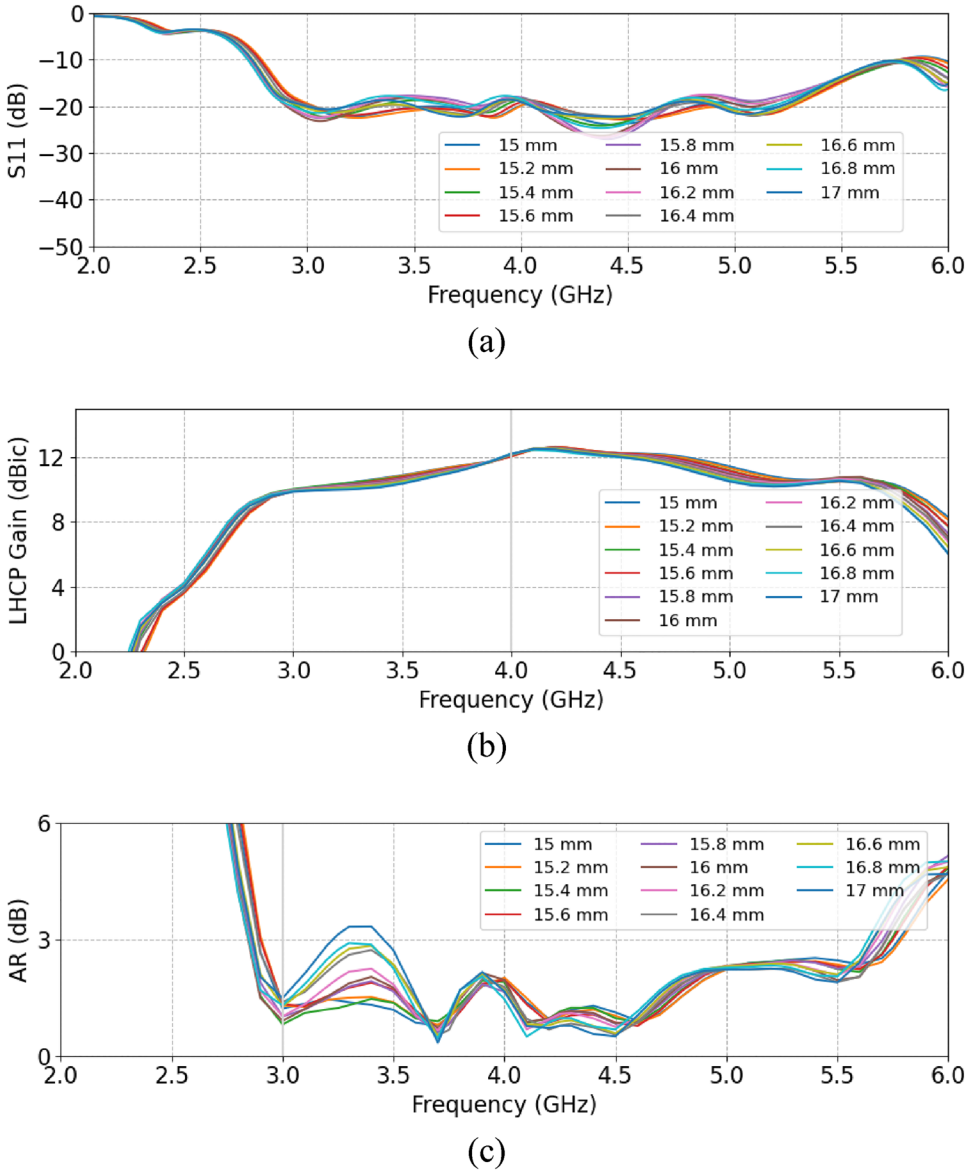

FIGURE 6 | Antenna performance as a function of air-gap height, H_1: (a) reflection coefficient, (b) gain, and (c) AR.

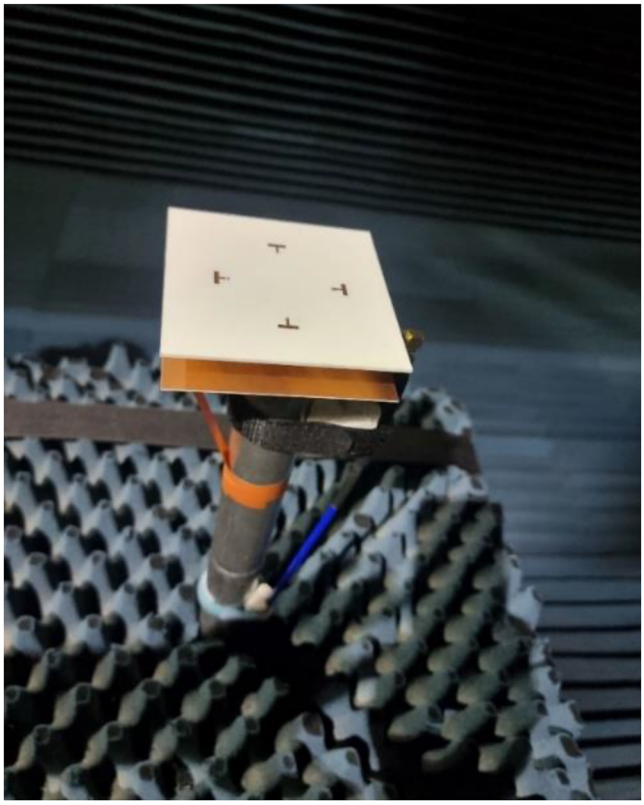

FIGURE 7 | Photograph of manufactured prototype antenna array mounted in a compact antenna range for radiation measurements.

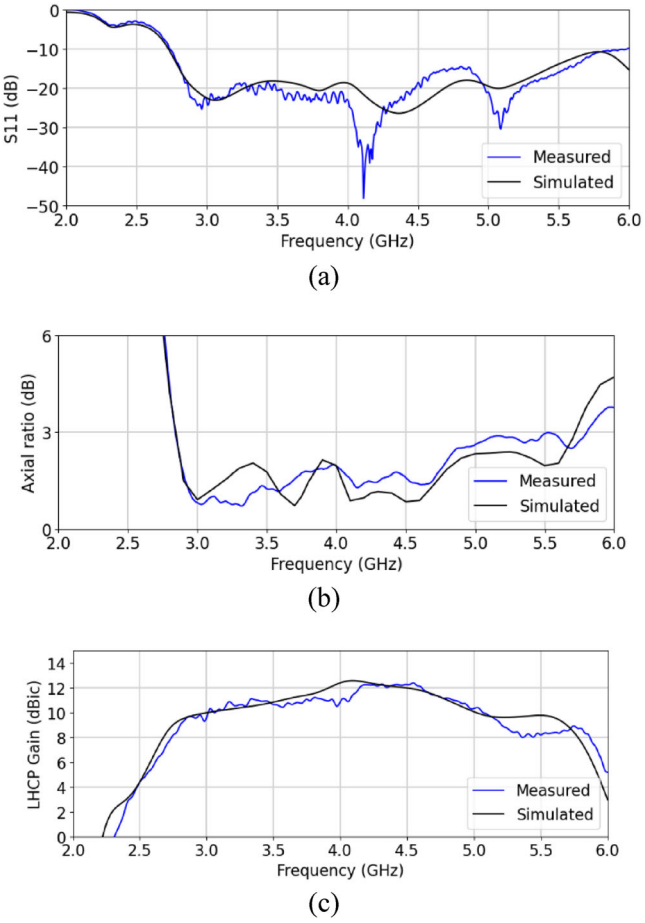

FIGURE 8 | Simulated and measured results of the CP ME dipole array: (a) S_{11}, (b) AR, and (c) LHCP gain.

the dipole and feed network dimensions, and the air-gap height, using CST Studio Suite. An IBW >75.0%, an ARBW of 67.0% and a maximum gain of 12.4 dBic were achieved for the antenna array. The 4-element CP ME dipole antenna array also has stable gain over a wide bandwidth, with less than 3 dB gain variation over the entire ARBW. The maximum gain improvement of the 2×2 array (relative to the single element) is 3.3 dB. The gain improvement of a sequentially fed array of four two-fold non-symmetrical elements can be significantly influenced by the element spacing (and hence mutual coupling) [13], which can cause the gain improvement to be significantly less than the theoretical 6 dB.

The radiation and total efficiency of the final design of the new CP ME dipole array were simulated and are shown in Figure 5 and was found to be well over 90% over a wide frequency band. The high simulated efficiency is confirmed by the low losses in the feed network, the good correlation between the measured and simulated gain, and small difference between the simulated gain and directivity of the antenna.

The air-gap height, H_1, was identified as a crucial parameter in the construction of the antenna. A sensitivity analysis was performed to determine the effect of H_1 on the performance of the antenna array. The variation of the reflection coefficient, the gain and the AR as function of the air-gap height are shown in Figures 6a–6c, respectively. It was concluded from the results that a manufacturing tolerance of $H_1 = 16 \pm 0.5$ mm would not degrade the performance of the antenna significantly.

3 | Measured Verification Results

A prototype of the proposed CP ME dipole antenna array was manufactured and measured. Figure 7 shows a photograph of the manufactured prototype of the CP ME dipole array in the compact antenna range of the University of Pretoria. A comparison of the simulated and measured results for the reflection coefficient, AR and boresight gain is shown in Figure 8a–c. The reflection coefficient and AR data correlation is very good. The maximum measured gain was only 0.2 dB lower than the simulated gain, but there was a larger gain difference at the high end of the band, which can be attributed to manufacturing/assembly tolerances and/or measurement error. Overall, there is sufficiently good agreement between the simulated and measured results to validate the design of the newly proposed antenna. Normalized simulated and measured radiation patterns of the CP ME dipole array (at 3 GHz, 4 GHz and 5 GHz) are presented in Figure 9a–f. It is only in the back lobe region that somewhat significant differences between the simulated and measured results can be observed. This is probably due to the measurement set-up in the compact antenna range, and specifically the presence of the pedestal at the back of the antenna that influenced the measured data. The radiation patterns of the proposed antenna remain stable, with well-formed main beams and low cross-polarization levels. The measured sidelobes were <−13 dB in the azimuth plane and <−18 dB in the elevation plane over

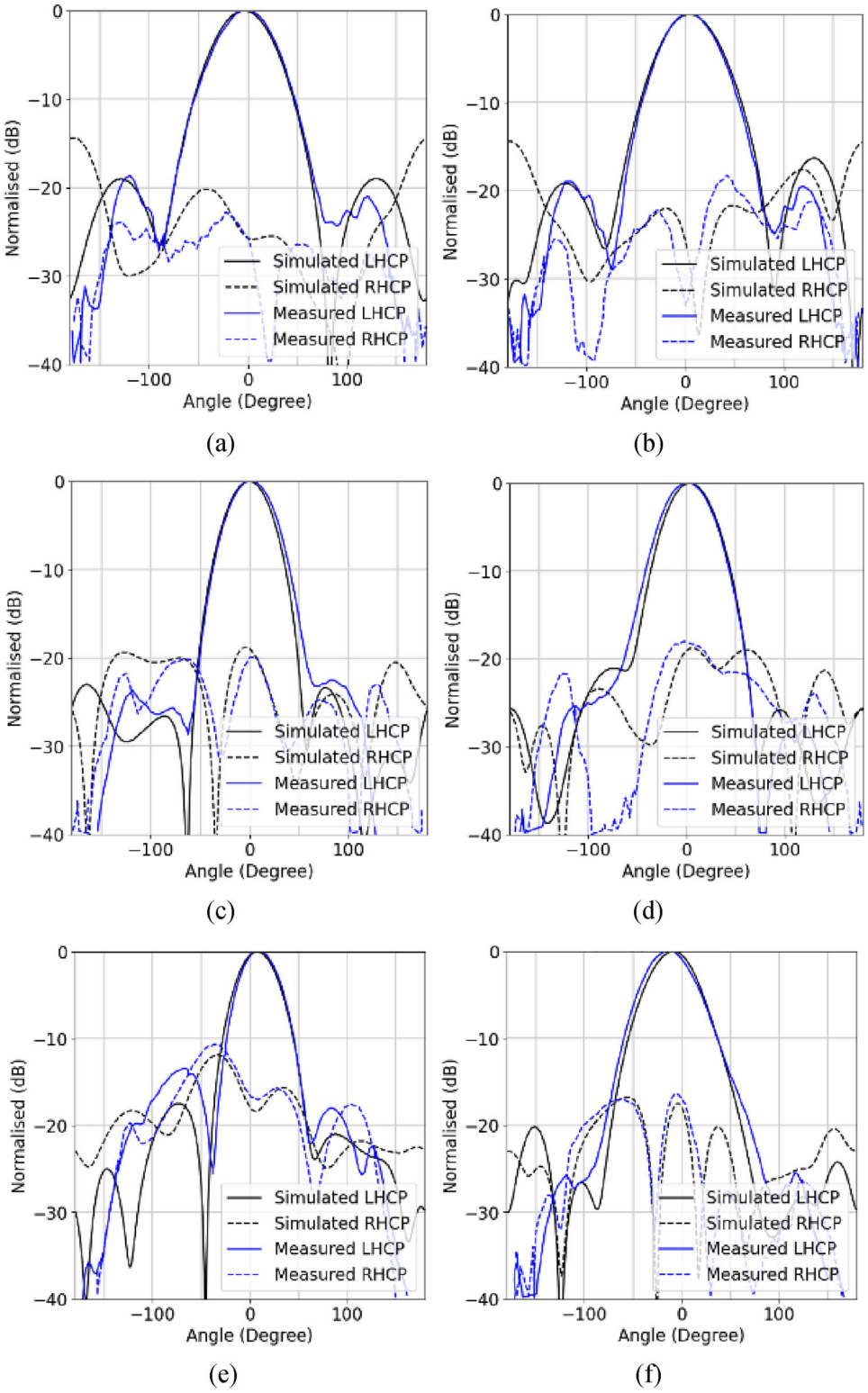

FIGURE 9 | Simulated and measured radiation patterns of the CP ME dipole array: (a) 3 GHz azimuth, (b) 3 GHz elevation, (c) 4 GHz azimuth, (d) 4 GHz elevation, (e) 5 GHz azimuth, and (f) 5 GHz elevation.

the entire bandwidth, and the maximum main beam squint from boresight was <11° in the azimuth plane and <14° in the elevation plane. The variation in 3 dB beamwidth in the azimuth plane was between 38°– 54°, and in the elevation plane between 46°– 53°. The back lobe was below −30 dB over the entire bandwidth.

A comparison of the results of the newly proposed antenna and that of previous related research is presented in Table 2. The second to last column lists the 3 dB GBW percentage defined as the frequency band where the antennas have less than 3 dB gain variation from the peak value. It is required that the other requirements must also be met in this band, that is,

TABLE 2 | Comparison between the proposed antenna and previous research.

Ref	IBW (%)	ARBW (%)	Max gain (dBic)	3 dB GBW (%)	Structure size and complexity (λ_L = wavelength at lowest frequency of the effective bandwidth)
[1]	70.2	51.5	9.9	51.5	$0.80\lambda_L \times 0.80\lambda_L \times 0.19\lambda_L$ Simple—printed structure above ground plane
[4]	53.7	51.1	12.6	45.0	$0.94\lambda_L \times 0.94\lambda_L \times 0.31\lambda_L$ Complex—printed feed structure with rectangular dielectric resonators
[5]	132.8	92.5	12.6	72.3	$1.41\lambda_L \times 1.41\lambda_L \times 0.13\lambda_L$ Complex—AMC, metal cone and another printed layer
[6]	69.1	57.7	8.5	57.7	$0.48\lambda_L \times 0.48\lambda_L \times 0.18\lambda_L$ Simple—printed structure above ground plane
[7]	66.4	57.3	11.3	53.6	$0.95\lambda_L \times 0.95\lambda_L \times 0.10\lambda_L$ Simple—printed structure above ground plane, and additional dielectric layer
[8]	95.5	94.4	7.9	87.2	$0.47\lambda_L \times 0.47\lambda_L \times 0.12\lambda_L$ Medium—printed structure above ground plane, with square metal columns
[9]	125.2	120.1	10.9	63.7	$1.11\lambda_L \times 1.11\lambda_L \times 0.25\lambda_L$ Complex—printed structure with complex cavity
This work	75.0	67.0	12.4	67.0	$0.94\lambda_L \times 0.94\lambda_L \times 0.17\lambda_L$ Simple—printed 2-layer structure

$|s_{11}| \leq -10$ dB, AR ≤ 3 dB, and stable radiation patterns. The last column in the table lists the electrical sizes of the antennas, and comments regarding the complexity of the manufacturing of the different antenna structures. The newly proposed antenna presented in this work has a better 3 dB GBW than all the listed antennas except for [5] and [8], but the new antenna is significantly smaller and less complex than that presented in [5] and has significantly higher gain than the antenna presented in [8]. The newly proposed antenna only has a slightly better 3 dB GBW than the antenna presented in [9], but the new antenna is also smaller and has a significantly higher gain.

4 | Conclusion

This paper presents a new wideband CP antenna array. The proposed CP antenna consists of four geometrically rotated, printed CP ME dipoles and a SP microstrip feed network on two printed substrates with an airgap in between. A prototype for operation for a centre frequency of $f_0 = 4$ GHz was manufactured and a usable bandwidth of 67% was achieved. The proposed CP antenna has a simple structure with a size of $0.94\lambda_L \times 0.94\lambda_L \times 0.17\lambda_L$ (relative to f_L, the lowest frequency of the effective bandwidth). No additional cavity or parasitic elements were required, which allows for simple design and construction of the antenna. The combination of compact size, wide CP bandwidth, high and stable gain (less than 3 dB variation across the band), and ease of manufacturing makes this antenna a suitable candidate for some modern communication applications that requires CP antennas.

Author Contributions

Elmien Coetzer: conceptualization, data curation, formal analysis, investigation, methodology, project administration, validation, visualization, writing – original draft, writing – review and editing. **Johan Joubert:** conceptualization, data curation, investigation, project administration, resources, supervision, validation, writing – review and editing. **Johann Wilhelm Odendaal:** conceptualization, data curation, investigation, project administration, resources, supervision, validation, writing – review and editing.

Conflicts of Interest

The authors declare no conflicts of interest.

Data Availability Statement

The data that support the findings of this study are available from the corresponding author upon reasonable request.

References

1. L. Cai and K.-F. Tong, "A Single-fed Wideband Circularly Polarized Cross-fed Cavity-Less Magneto-Electric Dipole Antenna," *Sensors* 3 (2023): 1067, https://doi.org/10.3390/s23031067.

2. P. S. Hall, J. S. Dahele, and J. R. James, "Design Principles of Sequentially Fed, Wide Bandwidth, Circularly Polarized Microstrip Antennas," *IEEE Proceedings H* 136 (1989): 381–389.

3. Y. Zou, H. Li, Y. Xue, and B. Sun, "A High Gain Compact Circularly Polarized Microstrip Array Antenna With Simplified Feed Network," *International Journal of RF and Microwave Computer-Aided Engineering* 29 (2019): e21964, https://doi.org/10.1002/mmce.21964.

4. S. Huang, H. Zhao, Z. Jiang, W. Yin, Z. Fang, and W. Chang, "Circularly Polarized Rectangular Dielectric Resonant Antenna With Sequential Phase Feed," in *Cross Strait Quad-Regional Radio Science and Wireless Technology Conference* (IEEE, 2019), 1–3.

5. R. Xu, S. S. Gao, J. Liu, J.-Y. Li, Q. Luo, and W. Hu, "Analysis and Design of Ultrawideband Circularly Polarized Antenna and Array," *IEEE Transactions on Antennas and Propagation* 68, no. 12 (2020): 7842–7853, https://doi.org/10.1109/TAP.2020.2998922.

6. H. Yang, Z. Guo, X. Li, Y. Zhang, X. Song, and S. Wang, "A Compact Circularly Polarized Crossed Dipole Antenna With Wide Bandwidth

Using Split Ring Resonator and Parasitic Patches," *ACES Journal* 38 (2023): 224–230.

7. W. J. Yang, Y. M. Pan, and S. Y. Zheng, "A Low-Profile Wideband Circularly Polarized Crossed-Dipole Antenna," *IEEE Antennas and Wireless Propagation Letters* 16 (2017): 2126–2129, https://doi.org/10.1109/LAWP.2017.2699975.

8. L. Wang, W.-X. Fang, W.-H. Shao, B. Yao, Y. Huang, and Y.-F. En, "Broadband Circularly Polarized Cross-Dipole Antenna With Multiple Modes," *IEEE Access* 8 (2020): 66489–66494, https://doi.org/10.1109/ACCESS.2020.2981050.

9. J. Fan, J. Lin, J. Cai, and F. Qin, "Ultra-Wideband Circularly Polarized Cavity-Backed Crossed-Dipole Antenna," *Scientific Reports* 12 (2022): 4569, https://doi.org/10.1038/s41598-022-08640-z.

10. J. Joubert and J. W. Odendaal, "Proximity Coupled Fed Wideband Printed Magneto-Electric Dipole Antenna," *IET Electronics Letters* 57, no. 22 (2021): 833–835, https://doi.org/10.1049/ell2.12287.

11. P. Mohammadi, M. Rezvani, and T. Siahy, "A Circularly Polarized Wide-Band Magneto-Electric Dipole Antenna With Simple Structure for BTS Applications," *AEU – International Journal of Electronics and Comm* 105 (2019): 92–97, https://doi.org/10.1016/j.aeue.2019.04.008.

12. D. Inserra, W. Hu, and G. Wen, "Design of a Microstrip Series Power Divider for Sequentially Rotated Nonuniform Antenna Array," *International Journal of Antennas and Propag* 2017 (2017): 9482979, https://doi.org/10.1155/2017/9482979.

13. A. K. Bhattacharyya, "Comparison Between Arrays of Rotating Linearly Polarized Elements and Circularly Polarized Elements," *IEEE Transactions on Antennas and Propagation* 56, no. 9 (2008): 2949–2954, https://doi.org/10.1109/TAP.2008.928783.